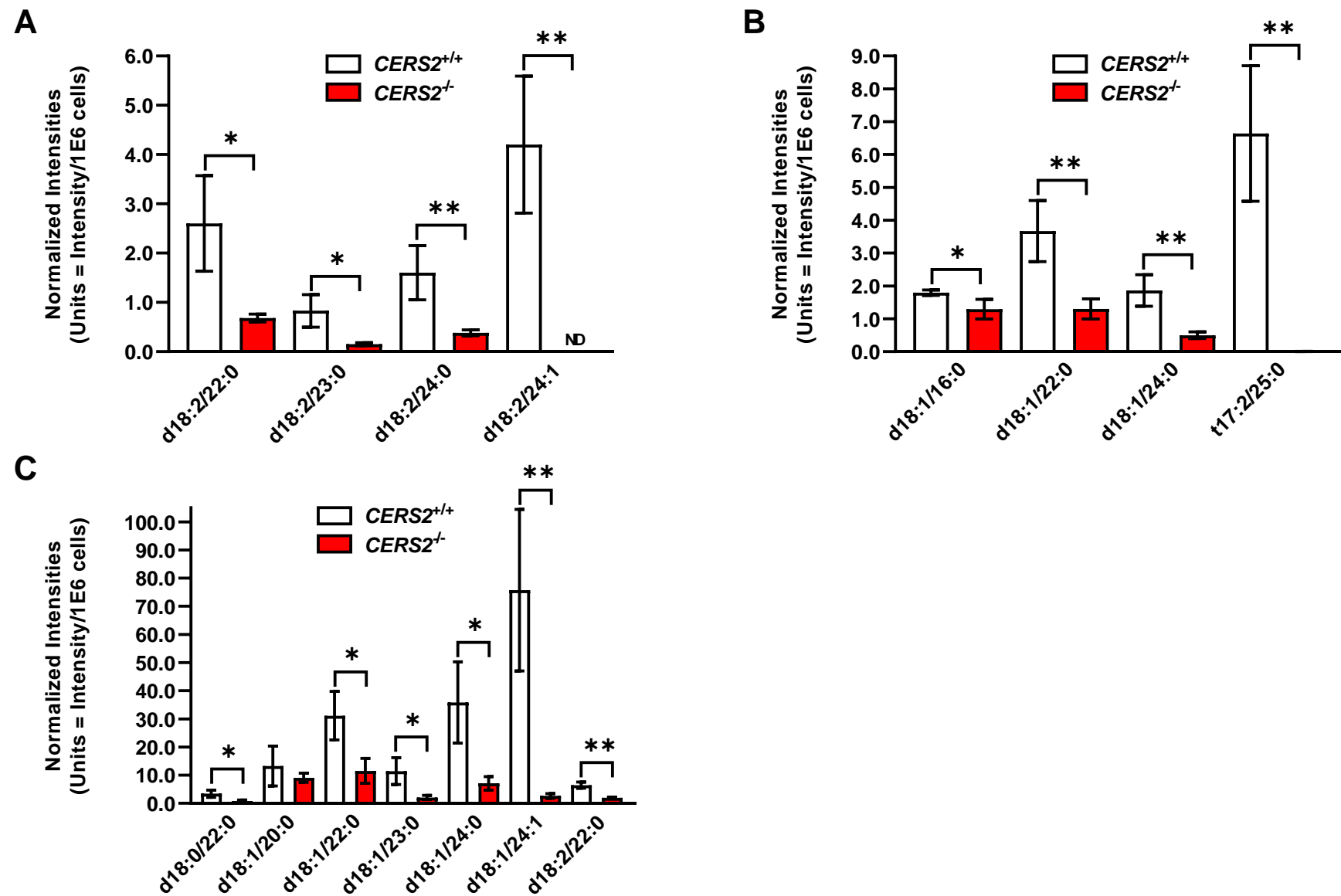
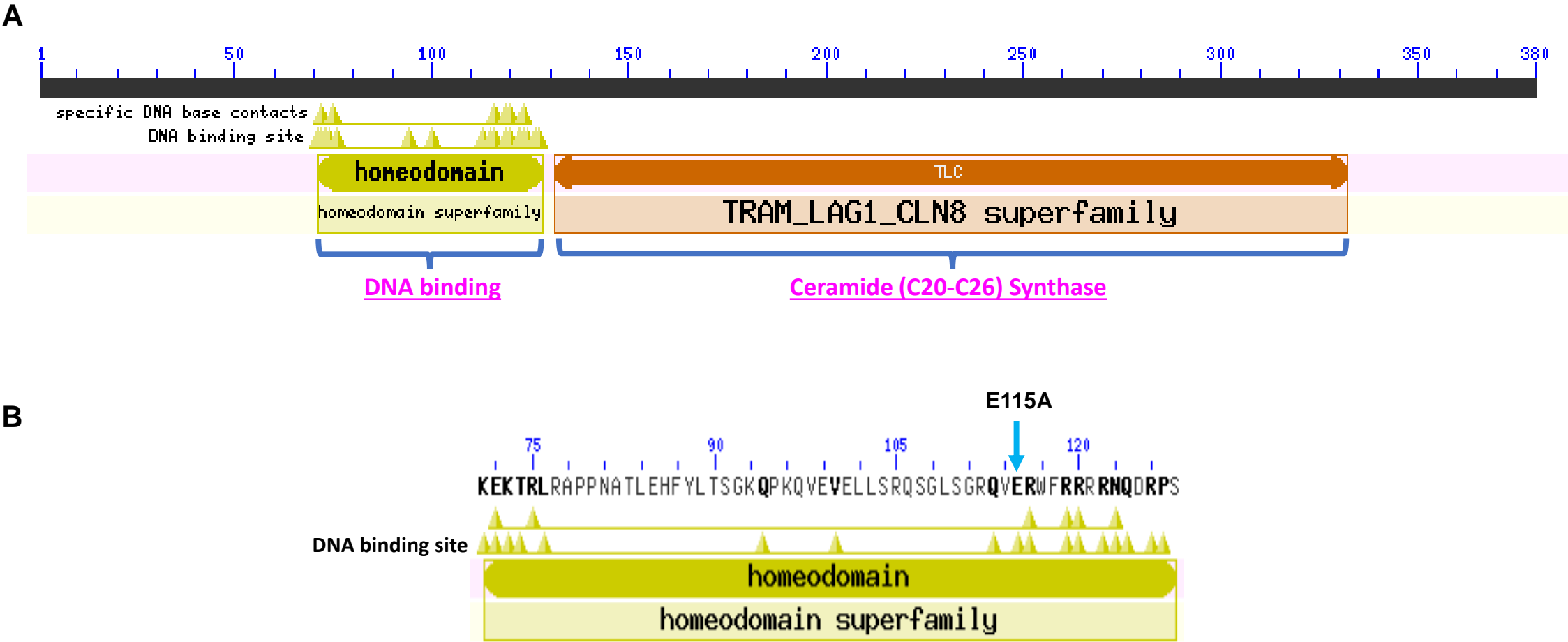


Supplemental Figure 1.



Sphingolipid levels for HepG2- $CERS2^{+/+}$ and HepG2- $CERS2^{-/-}$ cells treated with palmitate (500 μ M). **A**: Normalized intensities for VLCFA Cer d18:2 ceramides. **B**: Normalized intensities for LCFA and VLCFA hexosylceramides. **C**: Normalized intensities for VLCFA sphingomyelins. Data are expressed as mean \pm SD (n = 3). ND, not detected. * $P < 0.05$, ** $P < 0.01$.

Supplemental Figure 2.

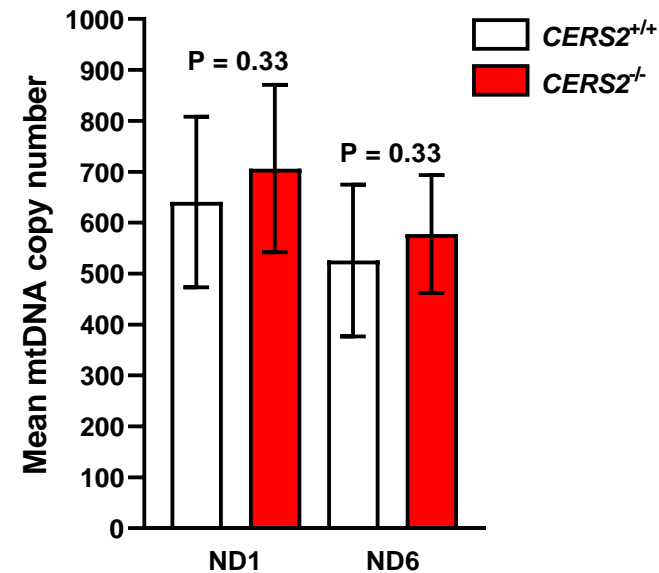


Schematics showing the conserved domains for the CERS2 protein. *A*: The TRAM, LAG1, CLN8 domain is important for acyl-CoA-dependent ceramide synthesis. The homeodomain is a DNA binding domain thought to be involved in regulating gene transcription. *B*: The rs267738 (E115A) missense variant changes an amino acid that may be involved in DNA binding. Figures were adapted from the NCBI conserved domain database (1-3).

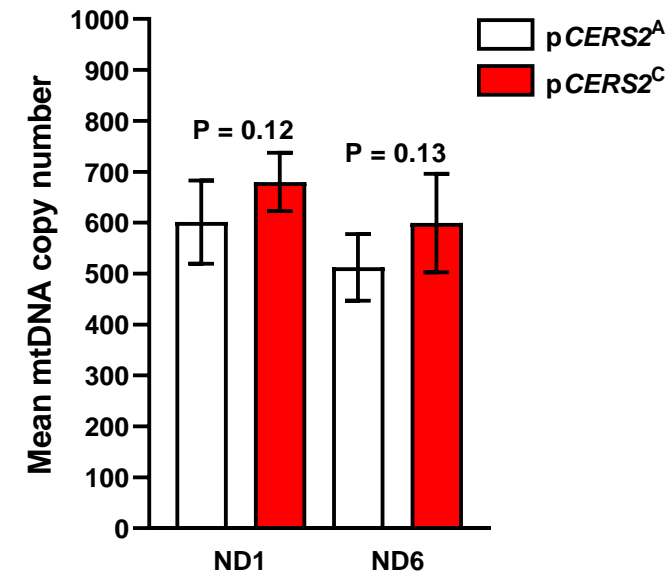
1. Wang J et al. (2023), "The conserved domain database in 2023", Nucleic Acids Res.51(D)384-8.
2. Lu S et al. (2020), "The conserved domain database in 2020", Nucleic Acids Res.48(D)265-8.
3. Marchler-Bauer A et al. (2017), "CDD/SPARCLE: functional classification of proteins via subfamily domain architectures.", Nucleic Acids Res.45(D)200-3.

Supplemental Figure 3.

A

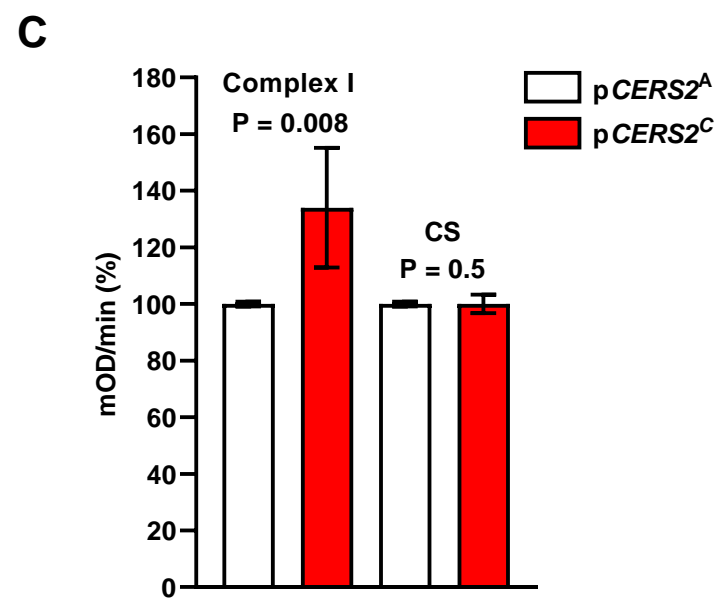
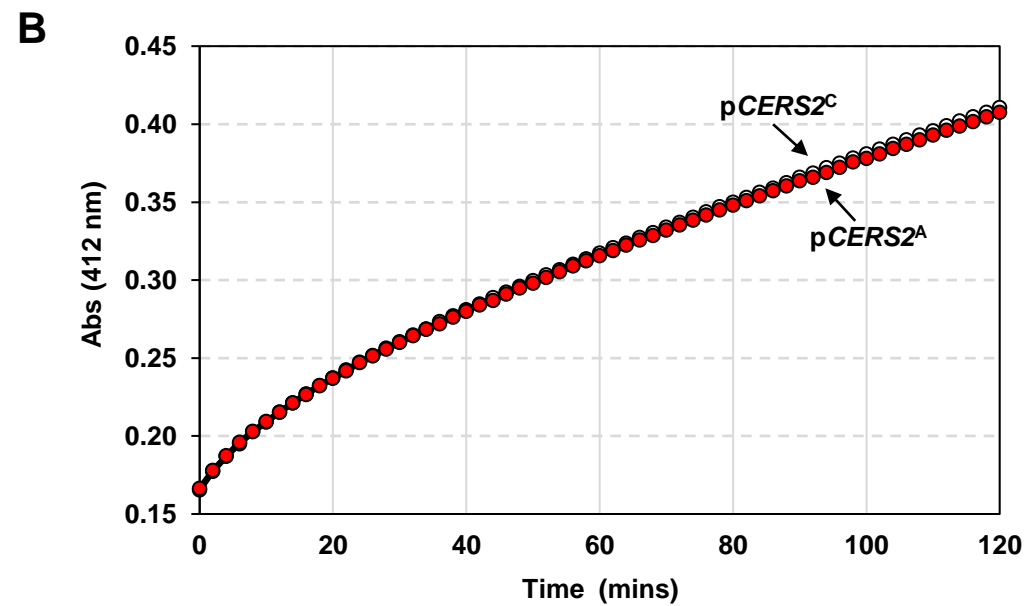
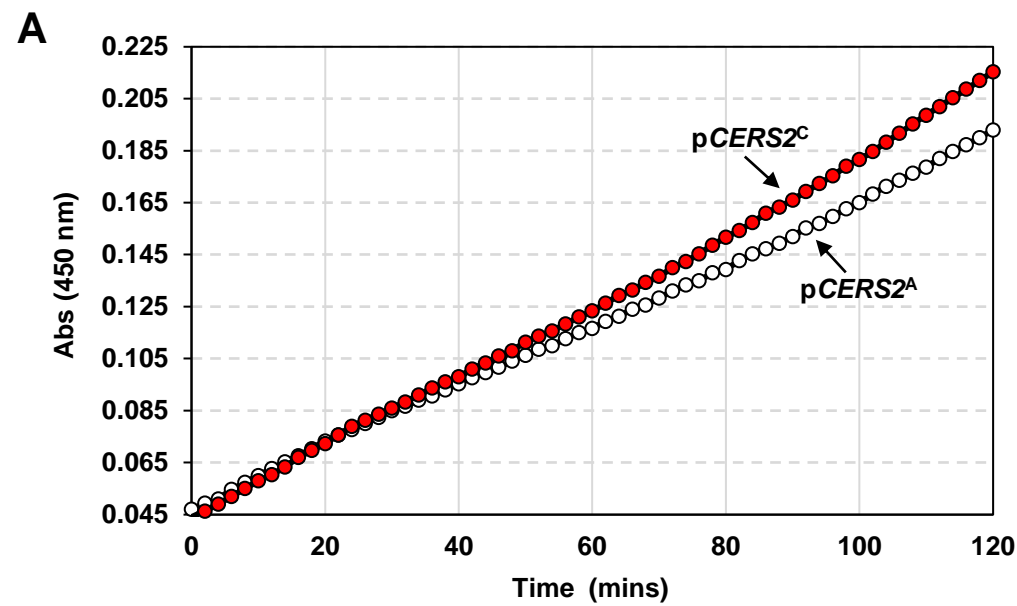


B



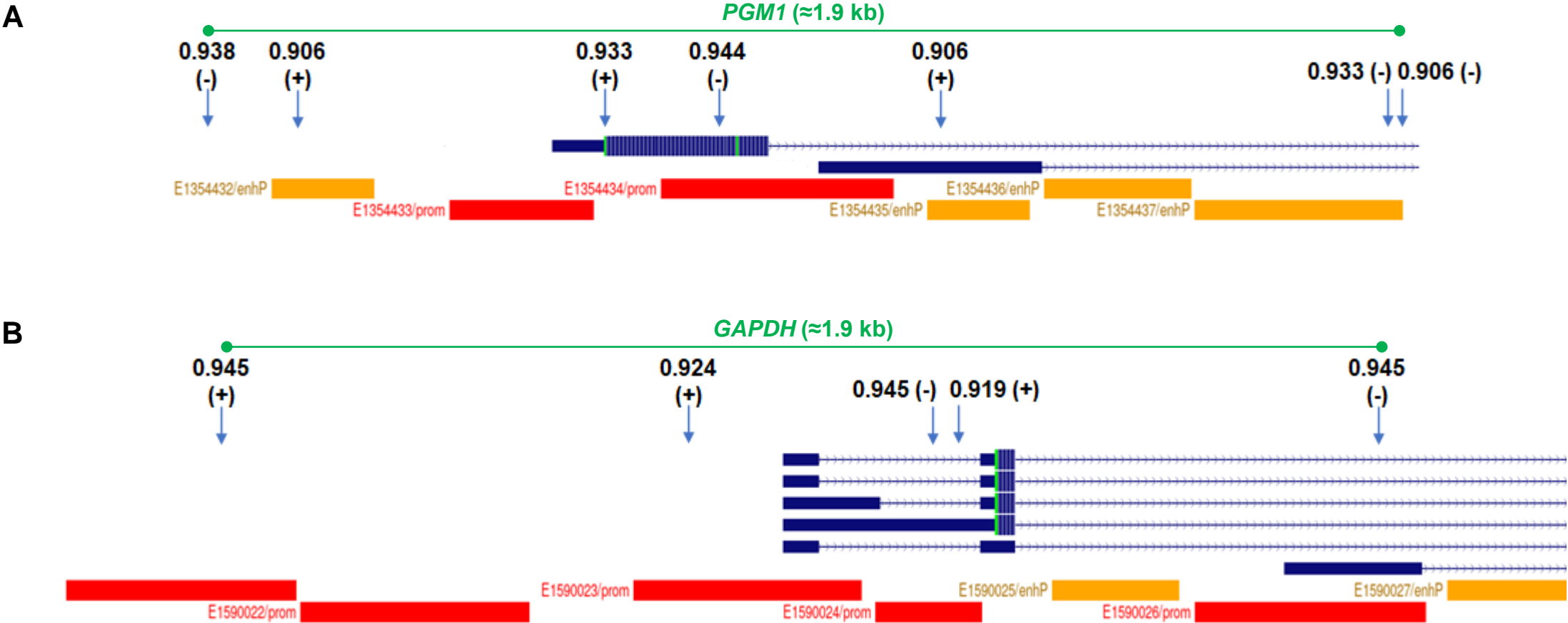
Mitochondrial DNA (mtDNA) copy number was determined by qPCR for two mtDNA genes, ND1 (H-strand) and ND6 (L-strand). *A*: Mean mtDNA copy numbers for HepG2-*CERS2*^{+/+} and HepG2-*CERS2*^{-/-} cells. ND1 and ND6 values were normalized to the nuclear (gDNA) reference gene TERT. *B*: Mean mtDNA copy numbers for HepG2-p*CERS2*^A and HepG2-p*CERS2*^C cells. ND1 and ND6 values were first normalized to the nuclear (gDNA) reference gene TERT and then with *CERS2* mRNA expression levels to account for transfection efficiency. Data (n = 3) are shown as mean ± SD.

Supplemental Figure 4.



Enzyme activities for NADH dehydrogenase (complex I) and citrate synthase for HepG2-pCERS2^A and HepG2-pCERS2^C cells. **A**: Representative plot from 4 independent experiments showing the change in OD 450 nm (enzyme activity) for complex I over time for HepG2-*CERS2*^{-/-} cells carrying either the pCERS2^A or pCERS2^C plasmid. **B**: Representative plot from 4 independent experiments showing the change in OD 412 nm (enzyme activity) for citrate synthase over time for HepG2-*CERS2*^{-/-} cells carrying either the pCERS2^A or pCERS2^C plasmid. **C**: Complex I and citrate synthase activities expressed as percent (%) change in absorbance per minute (mOD/min) for HepG2-*CERS2*^{-/-} cells carrying either the pCERS2^A or pCERS2^C plasmid. For the enzyme assays, equal amounts of protein were loaded in triplicate for each sample. Complex I activities were normalized to citrate synthase activities to account for mitochondrial content and *CERS2* gene expression levels to account for transfection efficiency. There were no differences in citrate synthase activities, suggesting that the difference in complex I enzyme activities is unlikely to be due to alterations in mitochondrial biogenesis. This is supported by the mtDNA copy number results shown in supplemental figure 1. Data in panel C are presented as mean \pm SD for 4 independent experiments performed on separate days.

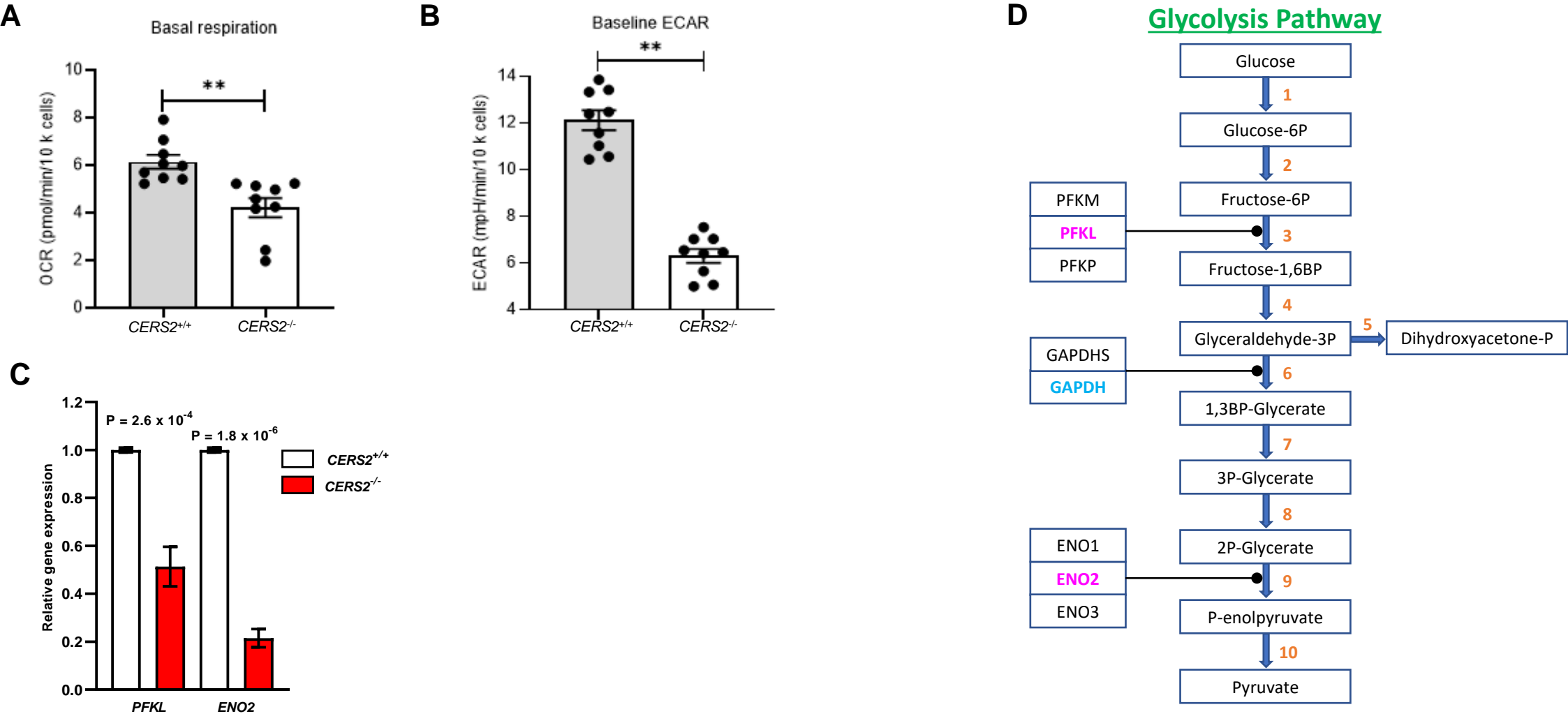
Supplemental Figure 5.



Schematics of A: *PGM1* and B: *GAPDH* 5' regions showing the location of predicted Schlank/lag1 (CerS) consensus binding sites (arrows) (1, 2). Schlank binding sites were determined using the JASPAR Core database and Insecta taxonomic group (3). Predicted Schlank binding sites with scores > 0.9 are shown. (+), predicted binding site located on the plus strand. (-), predicted binding site located on the minus strand. Figures were adapted from UCSC Genome Browser on Human (GRCh38/hg38).

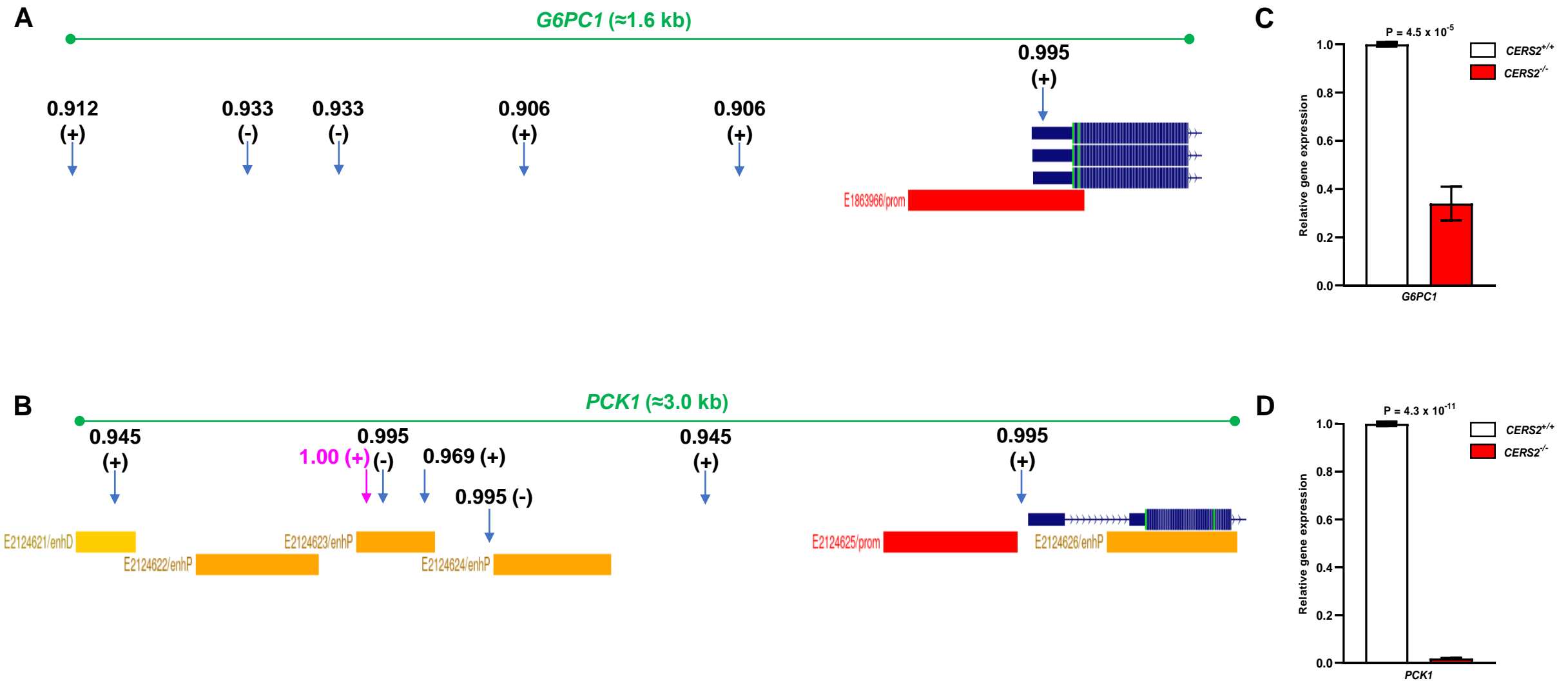
1. Noyes MB, Christensen RG, Wakabayashi A, Stormo GD, Brodsky MH, Wolfe SA. Analysis of homeodomain specificities allows the family-wide prediction of preferred recognition sites. *Cell*. 2008 Jun 27;133(7):1277-89.
2. Sociale M, Wulf AL, Breiden B, Klee K, Thielisch M, Eckardt F, Sellin J, Bülow MH, Löbbert S, Weinstock N, Voelzmann A, Schultze J, Sandhoff K, Bauer R. Ceramide Synthase Schlank Is a Transcriptional Regulator Adapting Gene Expression to Energy Requirements. *Cell Rep*. 2018 Jan 23;22(4):967-978
3. Castro-Mondragon JA, Riudavets-Puig R, Rauluseviciute I, Lemma RB, Turchi L, Blanc-Mathieu R, Lucas J, Boddie P, Khan A, Manosalva Pérez N, Fornes O, Leung TY, Aguirre A, Hammal F, Schmelter D, Baranasic D, Ballester B, Sandelin A, Lenhard B, Vandepoele K, Wasserman WW, Parcy F, Mathelier A. JASPAR 2022: the 9th release of the open-access database of transcription factor binding profiles. *Nucleic Acids Res*. 2022 Jan 7;50(D1):D165-D173.

Supplemental Figure 6.



A: The decrease in basal respiration for the BSA control (no exogenous palmitate) HepG2-*CERS2*^C cells (Fig. 4A, main text) was similar to the decrease in basal respiration we observed for BSA control HepG2-*CERS2*^{-/-} cells. The differential gene expression analysis suggests that the reduced OCRs for both groups of cells are due to alterations in the glycolysis pathway; however, the molecular mechanisms for impairment are different. C: The reduction in OCR for the HepG2-*CERS2*^C cells may be due to a decrease in *GAPDH* gene expression (Fig. 3, main text), whereas the lower OCR for the HepG2-*CERS2*^{-/-} cells may be a result of reduced expression of phosphofructokinase, liver type (*PFKL*) and/or enolase 2 (*ENO2*). B: The decrease in ECAR also indicates that glycolysis may be impaired for the HepG2-*CERS2*^{-/-} cells. D: Diagram showing the 10 steps of glycolysis. Differences in OCR and ECAR were tested using mixed models to account for repeated measurements from the same experiment. For *PFKL* and *ENO2* RT-qPCR, each sample was run in triplicate and relative gene expression levels were normalized using *ABL1*. Data are shown as mean \pm SD (n = 3). **P < 0.05.

Supplemental Figure 7.



Schematics of A: *G6PC1* and B: *PCK1* 5' regions showing the location of predicted Schlank/lag1 (CerS) consensus binding sites (arrows). Schlank binding sites were determined using the JASPAR Core database and Insecta taxonomic group. Predicted Schlank binding sites with scores > 0.9 are shown. (+), predicted binding site located on the plus strand. (-), predicted binding site located on the minus strand. Figures were adapted from UCSC Genome Browser on Human (GRCh38/hg38). C: and D: Knockout of *CERS2* in HepG2 cells that were not serum starved and not treated with insulin or dbCAMP resulted in a significant decrease in *G6PC1* and *PCK1* gene expression. For *G6PC1* and *PCK1* RT-qPCR, each sample was run in triplicate and relative gene expression levels were normalized using *ABL1*. Data are shown as mean \pm SD (n = 3).